LANGMUIR

Interface Components: Nanoparticles, Colloids, Emulsions, Surfactants, Proteins, Polymers

Sonochemically Assembled Photoluminescent Copper Modified Graphene Oxide Microspheres

Darya Radziuk, Lubov Mikhnavets, Anastasia Tkach, Ludmila Tabulina, and Vladimir Labunov

Just Accepted

ACS Publications

Sonochemically Assembled Photoluminescent Copper Modified Graphene Oxide Microspheres

Darya Radziuk,* Lubov Mikhnavets, Anastasia Tkach, Ludmila Tabulina and Vladimir Labunov

Belarusian State University of Informatics and Radioelectronics,

Laboratory of Integrated Micro- and Nanosystems,

6 P. Brovki Street, Minsk 220013 Belarus

*To whom correspondence should be addressed. E-mail: radziuk@bsuir.by

ABSTRACT

New accessible sonochemical assembly method is developed for the preparation of photoluminescent oil-filled silica@CuS/Cu$_2$O/CuO-GO microspheres with green, yellow and red colors of emitted light. This method is based on the ultrasonic emulsification of a biphasic mixture consisting of CuS/Cu$_2$O/CuO-graphene oxide (GO) nanocomposites with polyvinyl alcohol (PVA) (aqueous phase) and tetraethyl orthosilicate with sunflower oil (organic phase). CuS/Cu$_2$O/CuO-GO nanocomposites are composed of sonochemically formed three phases of copper: covellite CuS (p-type semiconductor), cuprite Cu$_2$O (Bloch p-type semiconductor) and CuO (charge transfer insulator). The photoluminescence property of microspheres results from the H-bridging between PVA and CuS/Cu$_2$O/CuO-GO nanostructures, light absorption ability of Cu$_2$O and charge transfer insulation by CuO. Substitution of PVA by S-containing methylene blue quenches fluorescence by enhanced dye adsorption on CuS/Cu$_2$O/CuO-GO because of CuS and induced charge transfer. Non-S-containing malachite green is in non-ionized form and tends to be in the oil phase, prohibiting the charge transfer on CuS/Cu$_2$O/CuO-GO.

Keywords. Sonochemistry, assembly, graphene oxide, photoluminescence, silica, encapsulation, dye, charge transfer, polyvinyl alcohol

1. Introduction

Biocompatible, biodegradable and nontoxic photoluminescent nanomaterials are highly desirable in drug delivery, cell imaging and in chemo/biosensing applications especially in cancer diagnostics, imaging and treatment.[1] Among these nanomaterials silica and graphene oxide (GO) have received great attention in the fields of composite materials, biosensing and drug delivery applications. SiO_2 provides monodispersity, higher specific surface area, controllable pore size and diameter, and versatile functionalization.[2] Incorporation of metals, metal/non-metal oxides or polymers into the SiO_2 network improves the interfacial contact, advances conducting pathways and suppresses the charge recombination.[3] GO has attracted great attention because of its unique properties and a two dimensional molecular structure.[4] Electronic properties of GO arise from the presence of both sp^3- and sp^2-hybridized carbon bearing various oxygen functional groups: hydroxyl, epoxy/carboxyl and carbonyl arranged on the basal plane and at the edges. However, pristine GO is a poor light emitter as its functional groups usually induce the nonradiative recombination by the transfer of their electrons to the holes present in sp^2 clusters producing localized electron−hole (e-h) pairs.[5] Currently much efforts are being made to improve the GO photoluminescence ability via the formation of hybrid complexes with –COOH groups, electron coupling of O atoms with the nearby C atom of the carbon lattice, protonation and deprotonation of functional groups, resulting in passivation or destruction of the nonradiative e-h recombination centers of GO.[6]

Variation of pH of the medium, modification with polymers and semiconductor nanostructures were used to enhance the charge transfer of GO and increase its fluorescence. Enhanced fluorescence resulted from the electronic excitation of carboxylate ions in GO (at low pH) and quasi-molecular GO-fluorophores (high pH).[7,8] Another strategy involved formation of

highly fluorescent hybrid nanocomposites with polymers (*e.g.* polyvinyl alcohol) and semiconductors (*e.g.* Cu_2O, CuO, CuS)[9,10] or heterojunction structures with ZnO and TiO_2.[11-13]

Various techniques have been used for the synthesis of such novel hybrid nanocomposites. Most of them require high temperature and pressure conditions, multistep synthesis and prolong reaction treatment. Alternatively, sonochemical method, which is based on acoustic cavitation,[14] is an efficient tool to form hybrid materials directly with GO (*e.g.* rGO/CuS, rGO/Cu_2O and CuO) and significantly improve photocatalytic[15] and catalytic,[16] selective sensing[17] and optoelectronic (incl. SERS)[18] properties, which make them useful in electronics, imaging and drug delivery applications.[19]

Sonochemical method is efficient, fast and convenient enabling assembly of substances at lower cost in a single step. It is a well-known method to produce oil-filled stable microspheres consisting of proteins, biomolecules and nanoparticles.[20-22] Ultrasonic emulsification was previously used for the preparation of liquid-filled GO microspheres by using a water-in-oil system[23] and assembly of preformed silica nanoparticles.[24] In a different study ultrasound is applied to the mixture of a silica precursor (*e.g.* tetraethyl orthosilicate) resulting in a silica sol formation acting as a passive matrix for a metal oxide particle entrapment and as an active phase for immobilization of organic hydrophobic dyes (*e.g.* phthalocyanines).[25] Ultrasonically encapsulated compounds retain their activity and spectroscopic properties, enabling transport in and out of the silica phase, but also some of them being left inside the silica pore.

In this work we show, that sonochemical functionalization of synthesized GO with copper sulfide and oxide can form $CuS/Cu_2O/CuO$-GO nanocomposites with advanced charge transfer properties (**Scheme 1A**). Sonochemical assembly of these nanocomposites by applying ultrasound to the biphasic mixture with polyvinyl alcohol in water and tetraethyl orthosilicate in

oil can produce photoluminescent microspheres at room temperature (**Scheme 1B**). In water our microspheres emit light of different colors: green, yellow and red. We attribute this light emitting property by charge transfer processes induced or quenched on the $CuS/Cu_2O/CuO$-GO nanostructures with polyvinyl alcohol at the silica:oil interface. For this we probe the interface by two structurally different organic dyes as model reactions: malachite green (MG) and methylene blue (MB). These dyes act as substitutes to the polyvinyl alcohol in the sonochemical assembly of microspheres. MG was selected because its electronic structure is sensitive to pH and can be switched between its localized ionized (at pH = 4) and delocalized non-ionized (at pH = 10) electronic forms.[26] MB was chosen because it belongs to the family of the electroactive dyes being used in chemical sensors and photoelectrocatalytic surfaces. MB as a cationic dye can be preferably adsorbed onto the S-containing surface depending on pH and electrostatic/hydrophobic interactions, leading to the enhancement or quenching of photoluminescence due to the charge transfer induced or prohibited on $CuS/Cu_2O/CuO$-GO nanostructures.[27]

2. Experimental Methods

Materials. Graphite was purchased from Imerys, France (detailed information about the graphite size and elemental composition can be found in supporting information). $Na_2S \cdot 9 H_2O$ (98 %), $CuCl_2 \cdot 2 H_2O$ (99 %), isopropanol (99 %), H_3PO_4 (85 %), $KMnO_4$ (98 %), H_2SO_4 (95 %), H_2O_2 (60 %), HCl (35 %), HNO_3 (40 %), C_2H_5OH (96 %), tetraethyl orthosilicate (TEOS) and polyvinyl alcohol (PVA) were obtained from Belreahim JSC (Belarus). Silver nitrate ($AgNO_3$, 99 %) and sodium borohydride ($NaBH_4$, 98 %) were obtained from Sigma-Aldrich Co. (Germany). Sunflower oil (refined, deodorized) was purchased from the Energy Group Inc. (Belarus). Distilled water (pH = 5.5, 5 μS/cm) was prepared by using a homemade distillation apparatus (Belarus). We synthesized graphene oxide (GO) using the Hummers method[28] (detailed information can be found in supporting information).

Sonochemical formation of $CuS/Cu_2O/CuO$-GO nanocomposites

In all our sonochemical experiments we used a homemade horn-type ultrasonic dispergator N.4-20 operating in a continuous mode at 20 kHz frequency with the 400 W maximal output power. This ultrasonic apparatus was specifically designed by Cavitation Inc. (Belarus) for the preparation of emulsions and suspensions. The ultrasonic intensity of this dispergator was calibrated by applying calorimetry (detailed information can be found in supporting information).[29]

Before the synthesis a powder of synthesized GO was dispersed in DI water (pH = 5.5) by sonication (18 W/cm^2 for 30 min) under ambient air in the ice-cooled water bath at a volume ratio of powder to water as 1:1. For the synthesis we took 1 mL of 1 mol·L^{-1} Na_2S aqueous solution which was added into the sonicated GO suspension. The mixture of Na_2S and GO was sonicated in a sealed thermostated beaker for 1 h at lower ultrasonic intensity 8 W/cm^2 at

T=60°C. After the ultrasonic treatment this mixture was cooled down to room temperature and the powder was precipitated by centrifugation at 4.293,12 x g for 30 min. The supernatant was removed and the precipitant was added by 5 mL of aqueous solution of 25×10^{-3} mol·L^{-1} CuCl$_2$. This solution was sonicated at 18 W/cm^2 for 2 h in a sealed thermostated beaker placed into an ice-cooled water bath. After that it was added by 1 mL of 1mol·L^{-1} Na$_2$S aqueous solution and sonicated again (18 W/cm^2 for 1 h). As the next step, this colloidal solution (pH = 12) was precipitated by centrifugation (4.293,12 x g) for 30 min and the supernatant was carefully removed. The precipitant was dispersed in DI water (pH = 5.5) and washed by repeated centrifugation until the final pH value of the colloidal mixture reached 5.5. This suspension was dried in the oven at 100°C and the fine black powder was obtained.

Sonochemical assembly of oil-filled silica@CuS/Cu$_2$O/CuO-GO microspheres

30 mL of aqueous 5 wt.% PVA solution was sonicated at 18 W/cm^2 for 30 min under air in the ice-cooled water bath in order to form a precursor emulsion solution. 5.5 mL of this PVA solution was added by aqueous CuS/Cu$_2$O/CuO-GO colloidal suspension at a volume ratio 1:1. Three types of aqueous mixtures were prepared: A) at pH = 6 (untreated); B) at pH = 2 by acidifying with aqueous 1 mol·L^{-1} HCl and C) at pH = 12 by addition of aqueous 44% KOH. The organic solution, consisting of 3.5 mL of TEOS and 3.5 mL of sunflower oil, was added by aqueous suspension resulting in the formation of two separate phases. The total volume of the biphasic mixture was 18 mL. Ultrasonic resonator's horn was placed at the interface of these two phases and the solution was sonicated at 27 W/cm^2 for 3 min under air. During sonication the solution was cooled by ice-water and the temperature during sonication maintained below 28° C. The final solution containing prepared microspheres was stored at room temperature, aged for full three days, separated from unreacted residues by using the separation flask and washed with

DI water for further characterization. For comparison, microspheres consisting of oil without TEOS were also sonochemically prepared according to the above described method. In this case, the organic solution of oil phase (no TEOS) was 7 mL. This method was also successfully applied to the preparation of air-filled silica@CuS/Cu$_2$O/CuO-GO microspheres (more details in supporting information).

Characterization

Dynamic light scattering (DLS) and ζ-potential (ZP) measurements were carried out on Malvern Zetasizer Nano ZS90 instrument with the use of a buffer solution of DI water (pH = 5.5) (more details in supporting information). DLS and ZP experiments were carried out on a 50 times diluted colloidal suspension of CuS/Cu$_2$O/CuO nanocomposites or 3 times diluted CuS/Cu$_2$O/CuO-GO microsphere solution. Each measurement took 10 s; the nanoparticle and microsphere distribution and electrophoretic curves were obtained by averaging ten measurements.

Samples of microsphere suspension were prepared for optical light phase contrast microscopy, by depositing the aqueous dispersions, previously washed with DI water, on a glass cover slip. The radius distribution of microspheres was analyzed by direct visualization via high speed camera connected to an optical light microscope (Planar MKI-2M): photographs were taken in real time and characterized by using Software imaging tool ScopeTek Scope Photo 3.1.312 (x86). The radius distribution diagrams were obtained by counting over 200 microspheres in each sample suspension. Two main microscope objectives with the A/F (aperture/focus) 0.08/48 (yellow) and 0.5/6 (white) with the resolution 936 pxl and 7290 pxl in 1 mm were used.

All samples were analyzed and characterized by using SEM S-4800 and energy dispersive X-ray fluorescence (Hitachi, Japan), UV-Vis absorbance in the range from 190 nm to 1200 nm by using HR-2000+ spectrometer (Ocean Optics) equipped with Ocean Optics DH-2000 white light source, FT-IR spectroscopy in the range from 400 cm^{-1} to 4000 cm^{-1} by using Zeiss Jena Specord-75IR (Germany).

Raman microscopy. Raman spectra were recorded by using 3D confocal Raman microscope Confotec NR500 from SOL Instruments Ltd. (Belarusian-Japanese joint venture "SOLAR TII") with Olympus UPlanFL N 40x/0.75 and Nikon CF Plan APO 100x/0.95 objectives. The Si wafer with the characteristic Raman line at 520 cm^{-1} was taken as a reference for calibration and basic alignment during integration time from 0.3 s to 1 s. For SERS measurements we prepared aqueous silver colloidal solution by using a method of chemical reduction of silver nitrate by sodium borohydride[30] and encapsulated silver nanoparticles into microspheres by using ultrasound (more details in supporting information). For Raman and SERS acquisition spectra a drop of microsphere solution was adsorbed on an aluminum plate followed by evaporation under ambient air for several hours. Two excitation wavelengths 473 nm and 633 nm with gratings 600gr/mm blazed at 500 nm and 600 nm were used to collect spectra from microspheres containing malachite green and methylene blue dyes. Aqueous solution of each dye was prepared at $1x10^{-4}$ mol·L^{-1} concentration in DI water (pH = 5.5) (more details in supporting information). Optical absorbance of these two dyes is the following i) MG: 316 nm, 426nm and 618 nm and ii) MB: 293 nm and 664 nm. The acquired Raman and SERS spectra were corrected for the baseline and background of the Si wafer.

3. Results and Discussion

We synthesized water soluble graphene oxide (GO) nanoparticles using the Hummers method[28] (**Figure S2A**). The success of graphite oxidation to form GO was confirmed by the appearance of an absorption peak at 237 nm with a shoulder near 295 nm, indicating the π–π^* transition of aromatic C=C bonds and the n–π^* transition of C=O bonds, in agreement with literature[31] (**Figure S2B**). Synthesized GO consists of carbon with lower amount than in the bulk graphite material (58.7 at.% vs 95.9 at.%), but with the concentration of oxygen being one order of magnitude larger (39.5 at.% vs 3.7 at.%) as a result of carbon oxidation (**Figure S3**, **Table S2 and S3**). Raman spectrum of nanoparticles exhibits distinct peaks at 1362 cm^{-1} and 1599 cm^{-1}, which are assigned to D (disordered carbon) and G (graphitic carbon) bands of typical GO (**Figure S4**). The intensity ratio of the G/D bands is about 1.02, indicating the synthesized GO of high quality. Indeed, the appearance of a broad triple band with more pronounced peaks corresponding to D+G and 2G$'$ also points out to a GO of better quality.

Sonochemical formation of CuS/Cu$_2$O/CuO-GO nanocomposites

After sonochemical synthesis final CuS/Cu$_2$O/CuO-GO nanocomposites acquired rough morphology containing nanostructures as revealed by SEM analysis (**Figure 1A and B**). EDX analysis of our nanocomposites shows lower concentration of carbon (33.4 at.%) and oxygen (18.2 at.%), and a higher concentration of sulfur (17.8 at.%) and Cu (28.1 at.%), suggesting the formation of CuS/Cu$_2$O/CuO in the GO nanostructure (**Figure S5**). The ξ-potential (ZP) of prepared CuS/Cu$_2$O/CuO-GO nanocomposites is slightly lower (-18 ± 9 mV) than the ZP value of synthesized GO nanosheets (-21 ± 7 mV) (**Figure S6A**). The DLS analysis reveals the bimodal distribution of synthesized GO nanosheets with two distinct peaks (100 nm and 490 nm) and a monomodal distribution of sonochemically prepared CuS/Cu$_2$O/CuO-GO nanocomposites

containing five times higher concentration of copper (**Figure S6B**). There is a small fraction of very small or much larger nanoparticles before sonication than after it, indicating that sonochemical method increases the homogeneous distribution of $CuS/Cu_2O/CuO$-GO nanocomposites, in agreement with the SEM analysis (**Figure 1A** and **B**).

As next, we performed Raman and X-Ray powder diffraction analysis in order to prove the presence of copper oxide and copper sulfide phases in synthesized GO nanocomposites (**Figure 1C and D**). The successful formation of covellite CuS[17] (p-type semiconductor) in the GO structure was confirmed by the appearance of a sharp Raman peak at 262 cm^{-1} (**Figure 1C**). Raman spectra also revealed the presence of cuprite Cu_2O (412 cm^{-1}), which is a Bloch p-type semiconductor,[16] and the successful formation of Cu bis-μ-oxo dimer[32] in GO nanocomposites due to the appearance of a sharp feature at 608 cm^{-1}. The formation of $Cu(OH)_2/Cu$ is less probable because of the absence of characteristic Raman bands at 298/347/591 cm^{-1} or at 297/344/629 cm^{-1} and 490/523/623 cm^{-1}.[33] FT-IR analysis also confirms the sonochemical formation of rather copper oxide and sulfide compounds in GO than metallic copper and $Cu(OH)_2$ (more details in supporting information with **Figure S7**).

X-Ray diffractograms of our synthesized GO nanoparticles and $CuS/Cu_2O/CuO$-GO nanocomposites are shown in **Figure 1D**. XRD patterns clearly indicate the GO phase due to the presence of a characteristic peak at 2θ = 12.0 arising from (001) plane. Predominant reflection (001) indicates that GO has a layered structure and its calculated interplanar spacing is 0.21 nm, in agreement with SAED measurements performed on finely powdered samples at Brookhaven national laboratory using synchrotron source.[34] This strong diffraction peak is broad as a result of very short range atomic coherence. In addition, the diffractogram also shows small peaks from graphene at 2θ = 25.0 from (002) plane and 2θ = 42.0 from (100) plane and their calculated

interplanar spacing values are 0.05 nm and 0.64 nm, indicating a loss of coherence between graphene-like layers. These smaller peaks are not sharp as a result of smaller in-plane structural coherence. Taking into account the van der Waals thickness of graphene, we can assume that synthesized GO nanoparticles consist of 4 layers, which can be stacked together into three larger structures forming individual sheets with increased thickness. The XRD pattern of CuS/Cu$_2$O/CuO-GO nanocomposites reveals multiple peaks of tenorite CuO with reflections (002), (111), (200) and (020) (databases amcsd Nr.0018812 and JCPDS card no. 80-1917), of cuprite Cu$_2$O with (110) plane (database amcsd Nr. 0007351 and JCPDF no. 78-2076), of covellite CuS with (101), (103), (110), (107), (108) and (116) planes (database amcsd Nr.0000065 and JCPDS card no. 78-0876), but only small peak from graphene (100), while the reflection (100) of GO disappears, indicating the formation of complexes between carbon and copper without intercalation of water molecules.

The presence of three phases (CuS, Cu$_2$O and CuO) in single GO nanocomposites demonstrates the efficiency of our sonochemical method in the preparation of p-type doped semiconductor nanocomposite with advanced charge carrier properties. For example, CuS can provide a significant density of valence-band delocalized holes without the need for intervening metal vacancies in the lattice. However, CuS is reluctant to incorporate cation vacancies due to the high activation energy required for their formation and the slow diffusion coefficient of cations within the lattice.[35] Cu$_2$O is known to produce water splitting into H$_2$ and O$_2$ under the action of visible light.[36] In addition, Cu$_2$O is intrinsically copper-deficient due to formation of copper vacancies that act as a shallow and efficient hole producers. The defect structure calculations of Cu$_2$O revealed that hydrogen can form a strongly bound complex with a copper vacancy. This hydrogen prefers not to occupy the center of the vacancy, but to move away from

the center closer to one of the two oxygen anions. Small fraction of Cu_2O can be formed by reduction of CuO at 773 K. Cu_2O is a classic exciton active semiconductor and CuO is known to act as a charge-transfer gap insulator. In this way the Cu_2O/CuO heterojunction can facilitate the electron-hole separation and significantly improve photo-to-chemical energy conversion efficiency. The enhanced photocatalytic activity can be improved due to the efficient electron transfer in Cu_2O-rGO-CuO via GO as a new and effective electron mediator providing large specific surface area.

Our sonochemically prepared CuS/Cu_2O-CuO-GO nanocomposites were further characterized by the UV-Vis absorption spectroscopy (**Figure S8**). UV-Vis absorption spectrum of colloidal GO suspension shows a broad plasmon peak near 237 nm (π-π* transition of C-C bonds in aromatic ring, 5.23 eV) and a pronounced shoulder at 295 nm (n-π^* transition of C=O bonds, 4.20 eV) due to the presence of the epoxide (C-O-C) and peroxide (R-O-O-R) bonds, in agreement with the predicted structure of density functional calculation.[34] In contrast, UV-Vis spectrum of colloidal CuS/Cu_2O/CuO-GO solution is dominated by the 1.5 times stronger and blue shifted plasmon peak at 230 nm (5.39 eV) and a weak shoulder near 340 nm (3.64 eV). In general, the π-π* plasmon peak depends on two conjugative effects related to the chromophore aggregation: i) nanometer-scale sp^2 clusters and ii) linking chromophore units such as C=C, C=O and C–O bonds. On one side, the change of the UV-Vis absorbance intensity can be explained by a conjugative effect related to chromophore aggregation: higher intensity indicates a few-layer (1-3) of GO and a smaller one – multilayer (4-10) of GO.[37] In this case our nanocomposite has a few-layer structure with the thickness of GO sheets increased by the presence of CuS/Cu_2O/CuO-GO nanostructures, in agreement with the XRD analysis (**Figure 1D**). On the other side, the blue shift of the plasmon peak of CuS/Cu_2O/CuO-GO nanocomposite can be

explained by the closer conjugation of copper compounds and GO nanosheets resulting in rapid electron transfer and increased transition energy. In addition, a blue shift can be also caused by introducing Cu vacancies into the CuS lattice resulting in generation of hole carriers. Ideally, a few-layer of GO should exhibit a single strong plasmon peak, but our CuS/Cu$_2$O/CuO-GO nanocomposite has a weak shoulder, which is smaller and red-shifted by 45 nm than a plasmon band of the synthesized GO. The red shift can be caused by the electronic conjugation within CuS/Cu$_2$O/CuO-GO nanosheets during the sonochemical synthesis.

In general, the electronic absorption spectrum of the Cu(II)$_2$ side-on peroxo-bridged species (*i.e.* Cu bis-μ-oxo) shows intense charge transfer band at 28000 cm^{-1} (3.47 eV), which is assigned as O$_2^{2-}$ π$_\sigma$* Cu(II) d$_{xy}$ transition involving transfer of e$^-$ density.[37] This charge transfer is indicative of a high degree of Cu-O covalency. A weak plasmon shoulder of our CuS/Cu$_2$O/CuO-GO nanocomposite is related to the charge transfer with the energy of 3.64 eV, indicating an energy increase on 0.17 eV involving O-Cu-O on the surface of GO nanosheets. If we compare plasmon peaks from GO (5.23 eV) and our CuS/Cu$_2$O/CuO-GO nanocomposite (5.39 eV), we can find an increase of the energy on 0.16 eV due to the presence of O-Cu-O or sulfide nanostructures on the GO surface.

As next, our new CuS/Cu$_2$O/CuO-GO nanocomposites were used for the sonochemical assembly of photoluminescent microspheres in the presence of polyvinyl alcohol (PVA), tetraethyl orthosilicate (TEOS) and oil.

Sonochemical assembly of CuS/Cu$_2$O/CuO-GO microspheres

Silica microspheres were assembled by ultrasonic emulsification of a biphasic mixture containing CuS/Cu$_2$O/CuO-GO nanocomposites and i) only TEOS, ii) the mixture of TEOS:oil or iii) only oil (**Figure 2**). Those microspheres, which were formed by

emulsification with TEOS (without oil) consisted of encapsulated air and changed their shape upon evaporation under ambient air (**Figure 2A**). However, they retain their morphology at 100°C and after additional sonication (30 min, 18 W/cm^2) in water. Most of the sonochemically prepared microspheres were stable colloidal solutions if consisted of encapsulated oil (**Figure 2B and C**). These oil-filled microspheres did not change their morphology and avoided coalescence or damage against repeated washing with isopropanol and centrifugation at 3.286,92 x g for 30 min, pointing out that the outer shell may be rigid by its composition.

a) Air-filled silica@CuS/Cu$_2$O/CuO-GO microspheres

We extended the sonochemical assembly method by using acidified (pH = 2) or alkaline (pH = 12) aqueous phase containing CuS/Cu$_2$O/CuO-GO nanocomposites in order to understand the mechanism of microsphere stability (**Figure 2A and D**). At low pH of aqueous phase no microspheres were formed and at alkaline conditions they appeared to be larger than those at pH = 5.5, but were destroyed during separation from the mother liquor solution. After incubation in aqueous solution at pH = 2 or at pH = 12 most of microspheres shrinked (**Figure S9**). Although microspheres were very stable during 7 days before separation from the mother liquor solution, they also shrinked after incubation in DI water at pH = 5.5. After careful observation of the morphology of these microspheres we noticed that their surface contained small particles of different phase contrast being clearly distinguishable by the optical microscope (**Figure 2D**). We assume that these particles may appear as a result of TEOS hydrolysis and its condensation in the form of small silica particles acting as nucleation centers during sonication. The appearance of these small silica nuclei was previously reported in the frame of the

proposed ultrasonic clustering model.[25] When microspheres were dispensed on a glass cover slip under ambient air some of them were entrapped in partially crystallized silica on top of them and retained their morphology during evaporation process. Addition of small amount of isopropanol resulted in separation of dried microspheres from the pieces of crystallized silica, but led to the microsphere collapse. When isopropanol was replaced by a drop of DI water (pH = 5.5), similar effects were observed. However, when a drop of TEOS was added, no visible changes of microspheres were noticed: no separation from crystallized silica, no shrinking and no collapse. The evaporation of the TEOS drop resulted in the formation of a microsphere shell with enhanced phase contrast and a transparent core, in agreement with the ultrasonic clustering model. However, this shell developed visible defects, was ruptured and collapsed during evaporation under air.

b) *Oil-filled PVA@CuS/Cu$_2$O/CuO-GO microspheres*

The stability of microspheres was significantly improved when oil and polyvinyl alcohol (PVA) were added into the biphasic TEOS : water mixture containing CuS/Cu$_2$O/CuO-GO nanocomposites (**Figure 2B and E**). In the aqueous phase PVA acted as surface active material resulting in the formation of a precursor emulsion system, which consisted of the hydrophobic part pointing towards the core and leaving outer OH$^-$ groups in the bulk aqueous solution. PVA is known to contribute to the formation and stability of colloidal suspension by lowering the interfacial tension, increasing the surface elasticity (viscosity) and electric double layer repulsion, enhancing the tighter packing of hydrophobic groups at the oil/water interface. The presence of sunflower oil in the TEOS:water mixture or in water was essential for the enhanced stability of these microspheres, in agreement with the previous findings of dodecane or soya bean oil[20-22]

(**Figure 2C and F**). Indeed, without oil (with TEOS) most microspheres quickly dried and collapsed during evaporation independently on the presence of PVA. In contrast, our sonochemically formed oil-filled microspheres were stable upon drying under ambient air and after 2 h of heating at 100°C, retained their shape and could be dispersed in water without collapse or shrinking (**Figures 2B and C**). We noticed no defects of the microsphere morphology or its damage after heating at 100°C and assumed that the oil-core of microspheres was protected by the densely formed silica@CuS/Cu$_2$O/CuO-GO composite shell. In addition, no damage of these microspheres was revealed after repeated centrifugation cycles, mechanical shaking and stirring.

The composition of our sonochemically prepared microspheres was studied by Raman microscopy (**Figure S10**). Raman spectra of oil-filled microspheres containing silica and CuS/Cu$_2$O/CuO-GO nanocomposites showed the presence of D band at 1362 cm^{-1} and G band being shifted to higher frequency range at 1604 cm^{-1}. Both peaks appeared with lower intensity than in nanocomposite and became broader with a small peak in between at 1442 cm^{-1} due to the presence of liquid TEOS (SiOC$_2$H$_5$)$_4$, indicating that CuS/Cu$_2$O/CuO-GO is indeed incorporated into the silica matrix.[38] This silica-GO matrix is in close contact with the oil phase due to the appearance of a weak shoulder at 1655 cm^{-1} arising from the cis double bond stretching of $_v$(C=C).[39] Oil-filled microspheres without CuS/Cu$_2$O/CuO-GO are also composed of silica because Raman spectra reveal distinct peaks from the oil and liquid (SiOC$_2$H$_5$)$_4$ phases.

c) Mechanism of oil-filled microsphere sonochemical assembly

As next, we examined the effect of pH of aqueous phase in order to find out the mechanism of sonochemical assembly of oil-filled CuS/Cu$_2$O/CuO-GO microspheres and

studied their size dependence on the type of organic phase and ultrasonic intensity. In particular, we were interested in whether electrostatic or hydrophobic interactions or covalent bonds play the dominant role.

d) Effect of pH

Two types of microspheres were prepared: i) with TEOS:oil mixture at a volume ratio 1:1 and ii) with only oil (no TEOS). Overall, only few microspheres, which were formed with oil as a single organic phase, appeared with larger size (70 μm-120 μm) depending on pH. At pH = 2 some microspheres acquired increased diameter (110 μm ± 10 μm) and at pH = 5.5 – smaller size (**Figure 2G**). However, the majority of microspheres obtained radius smaller than 10 μm and constituted a larger fraction of even smaller microspheres (1-2 μm) at all pH values. We noticed the following dependence of microsphere's radius versus pH value: the radius of most microspheres was gradually decreased from low to high pH values. The influence of the pH value on the size distribution of microspheres can be explained by the hypothesis that GO is an amphiphile with a largely hydrophobic basal plane and hydrophilic edges being pH dependent.[40] In addition, GO can also act as an emulsifier and a colloidal surfactant. According to this hypothesis the edge –COOH groups can be reversibly protonated (at low pH = 2) and become less water soluble or can be charged (at high pH = 12) becoming more hydrophilic. Therefore GO has a tendency to migrate towards the oil phase at lower pH and to water at a higher pH. At a higher pH the aqueous phase is saturated with GO and PVA precursor emulsion with outer head groups pointed in the bulk aqueous solution. Therefore, GO can reversibly alternate between water and oil phases, and this property of GO can be useful for phase transfer processes during ultrasonic emulsification. Overall, emulsions can be easily formed in

solutions with higher viscosity, resulting in spheres with larger radius. In our biphasic system the viscosity decreases in the following order: oil (68 mPa·s) $\rightarrow$ TEOS : oil mixture (about 66 mPa·s) $\rightarrow$ water (1 mPa·s). We can assume that at lower pH our CuS/Cu$_2$O/CuO-GO nanocomposites are more hydrophobic, facilitating the emulsification of oil phase, resulting in CuS/Cu$_2$O/CuO-GO microspheres of larger radius. At higher pH our CuS/Cu$_2$O/CuO-GO nanocomposites are more hydrophilic and emulsification is less efficient due to the lower viscosity of water, resulting in CuS/Cu$_2$O/CuO-GO microspheres of smaller radius.

e) Effect of aging

We examined how the morphology of our oil-filled silica@CuS/Cu$_2$O/CuO-GO microspheres was developed during a prolonged period of time of aging (from several days to a month) and plotted the size distribution curve (**Figure 2G**). We noticed that the average number of microspheres with larger diameter decreased from being 155 to 135 after 5 days of aging at room temperature under ambient air. This can be attributed to the formation of a denser silica network leading to shrinking of microspheres as a result of excess of Laplace pressure. Indeed, we observed the formation of silica gel-like structures after aging of our microsphere suspension for a month.

f) Effect of ultrasonic intensity

We also studied the effect of ultrasonic intensity on the formation mechanism of our oil-filled silica@CuS/Cu$_2$O/CuO-GO microspheres. At very low intensity (8.23 W/cm^2) no microspheres could be formed independently on pH value. At higher intensity (27.73 W/cm^2) large, medium and small microspheres were produced, but at 36.98 W/cm^2 mostly very small microspheres were prepared (**Figure 2G**). The amount of microspheres

with smaller diameter was larger at higher ultrasonic intensity although a small fraction of larger microspheres was also present. Similar effects on the size distribution of microspheres were observed in the sonochemical formation of proteinaceous microspheres,[20-22] in agreement with the acoustic emulsification model.[41] In the presence of TEOS, a silica precursor, the hydrolysis and condensation processes take place within several minutes of sonication. The hydrolysis reaction involves the replacement of alkoxy groups (OR) by hydroxo ligands (OH) followed by silica formation in a subsequent condensation. The rate of hydrolysis is slower at pH = 7, but can be significantly increased at acidic (GO is more hydrophobic) or alkaline (GO is more hydrophilic) conditions. In contrast, the rate of condensation is much higher at pH = 7, but is decreased at acidic or alkaline conditions. In our experiments the pH of TEOS solution was 7, facilitating the condensation, leading to cross-linking and formation of a dense structure of silica network. We suggest that those microspheres, which were prepared using aqueous GO phase at lower pH would force more hydrophobic GO towards the organic TEOS:oil phase and speed up the hydrolysis rate, resulting in the formation of more homogeneous microspheres with loose and open structure that collapses upon drying. The nonpolar alkyl chains of TEOS molecules can slowly diffuse through PVA precursor emulsion resulting in the formation of $CuS/Cu_2O/CuO$-GO-PVA silica sol at the oil : water interface followed by the growth of a silica shell during the hydrolysis and condensation cycles.

Photoluminescence of oil-filled PVA/$CuS/Cu_2O/CuO$-GO microspheres

We noticed that sonochemical assembly of oil-filled PVA/$CuS/Cu_2O/CuO$-GO microspheres led to intense photoluminescence from the microsphere's shell during the

exposure to the visible light (**Figure 3**). Many of these microspheres acquired a surrounding shell of green color, which was changed into yellow and red and then back to green again (**Figure 3A**). Overall not all of microspheres appeared to be highly photoluminescent and we found this optical property to be dependent on pH, the presence of TEOS and PVA. At higher pH (*e.g.* 5.5 or 12) and without TEOS only few oil-filled PVA/CuS/Cu_2O/CuO-GO microspheres were photoluminescent. No photoluminescent microspheres appeared at acidic conditions without TEOS. We suggest that the hydrophilicity of CuS/Cu_2O/CuO-GO nanocomposites and their interaction with PVA may play a role in the mechanism of photoluminescence. At pH = 5.5 CuS/Cu_2O/CuO-GO nanocomposites are amphiphilic and at higher pH they become more hydrophilic, facilitating interaction with PVA in the aqueous phase during sonication. In addition, at higher pH photoluminescence can arise due to the electronically excited carboxylate ion of GO.[42,43] However, at low pH CuS/Cu_2O/CuO-GO is more hydrophobic, facilitating the interaction with the oil phase, which may lead to the quenching of photoluminescence.

In addition, we also observed very intense photoluminescence from oil-filled PVA/CuS/Cu_2O/CuO-GO microspheres, which were sonochemically prepared with TEOS and dried for 2h at 100°C (**Figure 3B**). These microspheres exhibited intense pale yellow color independently on pH. We suggest that with TEOS the viscosity of the oil phase decreases facilitating the hydrolysis involving CuS/Cu_2O/CuO-GO and PVA during sonication. In this case the hydrophilicity of CuS/Cu_2O/CuO-GO becomes less significant. Heating of these microspheres at 100°C may lead to the removal of excess of water from the microsphere's shell containing silica network, PVA and CuS/Cu_2O/CuO-GO nanocomposites and induce the radiative processes.

Only those oil-filled PVA/CuS/Cu$_2$O/CuO-GO microspheres, which were prepared without TEOS, changed intense colors of their shells such as green, yellow and red, while their core remained black during exposure to the visible light (**Figure 3C**). These microspheres did not acquire different colors immediately after their preparation, but initially exhibited only green color and then sequentially changed it into yellow and red, and then back to green again. We suggest that light first interacts with the water molecules surrounding the microsphere's shell and leads to the partial evaporation of their thin layers resulting in excitation of the shell containing CuS/Cu2O/CuO-GO and PVA. We assume that diffusion processes and Brownian motion of microspheres in the aqueous solution may contribute to the change in the interaction with the light and main charge transfer mechanisms. We exclude the electrostatic interactions in the formation mechanism of microspheres because the surface charge of cavitation bubbles, PVA precursor emulsion and CuS/Cu$_2$O/CuO-GO nanocomposites is negative. Interaction of PVA with CuS/Cu$_2$O/CuO-GO nanocomposites may occur via the formation of hydrogen bridges. It was reported that hydrogen bonds can be formed between the hydroxy groups of PVA and GO due to the supramolecular organization of GO-PVA complex, which is facilitated in acidic medium (pH = 4) during prolonged sonication (2 h).[42] This PVA-GO hybrid is highly photoluminescent and exhibits intense green light because of passivation by hydrogen bonding. In our sonochemical assembly method we used pH = 12 and sonication for only 3 min in order to prepare green-light emitting PVA-CuS/Cu$_2$O/CuO-GO microspheres. In a basic medium CuS/Cu$_2$O/CuO-GO nanocomposites become more hydrophilic and their interaction with the –OH groups of PVA can be easier during sonication and may lead to the formation of a joint photoluminescent complex at the oil/water interface. On the other hand, it was reported that Cu$_2$O exhibits yellowish-red color as a result of

light absorption before thermal oxidation under air.[36] However, after thermal oxidation it changes its color to black, indicating the formation of CuO. This color change is reversible as a result of a bilayer structure that is composed of an inner Cu_2O layer and an outer CuO layer with a possible Cu_2O/CuO heterojunction between the two layers. In our PVA-CuS/Cu_2O/CuO-GO microspheres the color of the emitted light reversibly changes from green to yellow and to red and back to green in each photoluminescent microsphere during exposure to the visible light for several min under air. We assume that the shell of our highly photoluminescent microspheres may consist of sonochemically formed PVA-CuS/Cu_2O/CuO-GO complex via H-bonding and the color change is due to the light absorption by Cu_2O avoiding reactive oxidation species (ROS) with the CuO acting as a charge transfer insulator.

As next, we examined the efficiency of our sonochemical assembly method for the encapsulation of organic dyes into the silica@CuS/Cu_2O/CuO-GO microspheres without PVA.

Dye encapsulation properties of oil-filled silica@CuS/Cu_2O/CuO-GO microspheres

The efficiency of ultrasonic emulsification was examined by Raman microscopy through an organic dye encapsulation into the oil-filled silica@CuS/Cu_2O/CuO-GO microspheres (**Figure 4**). In our study we used two organic dyes: i) methylene blue (MB) and ii) malachite green (MG) as model reactions to probe the charge transfer at the silica@CuS/Cu_2O/CuO-GO:oil interface. These two dyes have different chemical structures: MB contains sulfur and MG does not. MB absorbs energy directly from a light source and then transfers this energy to molecular oxygen, generating singlet oxygen ($^1O_2$).[44] Singlet oxygen is electrophilic and can oxidize electron-rich double bonds. Electron transfer in photoactivated MB can produce reactive oxygen species, including hydroxyl radicals and

hydroperoxides. In contrast, MG can exist in two ionic forms—as the dye salt and as the carbinol or pseudobase.[45] Cations of MG covalently combine with hydroxyl ions to produce a non-ionized pseudobase. This pseudobase has a much greater liposolubility than the cation. In addition, MG is strongly ionized at lower pH (*e.g.* 100% at pH = 4.0) and is in non-ionized form at higher pH (*e.g.* pH = 10.0), resulting in its weak or no interaction with OH⁻ in basic medium and higher tendency towards the organic phase, which is oil in our system. In contrast to MG, the presence of CuS and sulfide in the carbon lattice of $CuS/Cu_2O/CuO$-GO nanocomposite may facilitate the adsorption of S-containing MB and induce the charge transfer process. In oil-filled silica@$CuS/Cu_2O/CuO$-GO microspheres Raman spectra revealed multiple peaks from MB[25] and small peaks from liquid TEOS ($Si(OC_2H_5)_4$) as well as D and G bands of GO, indicating the successful encapsulation of MB into the silica-GO network of microspheres and not in its oil phase (**Figure 4A**). As a control, we also prepared dye encapsulated silica microspheres without $CuS/Cu_2O/CuO$-GO nanocomposites. In this case we observed a strong fluorescence continuum with small multiple peaks from MB and $Si(OC_2H_5)_4$ on the top of it due to the interaction of encapsulated dye with the silica network. We suggest that the fluorescence quenching may result from an induced charge transfer on the $CuS/Cu_2O/CuO$-GO surface with adsorbed MB. We assume that the majority of MB molecules are adsorbed on the $CuS/Cu_2O/CuO$-GO surface because MB is a cationic dye and the nanocomposite is negatively charged, and due to the presence of sulfur, which additionally favors the dye deposition on GO.

In contrast to MB, Raman spectra[39] show several small peaks arising from symmetric rock in *cis* double bond $_\delta$(=C-H) at 1266 cm⁻¹, in-phase methylene twist at 1302 cm⁻¹ and

cis double bond stretching ν(C=C) at 1660 cm^{-1}, indicating that MG is ultrasonically encapsulated rather in the oil phase than in the silica@CuS/Cu$_2$O/CuO-GO shell (**Figure 4B**). In addition, no fluorescence was observed from MG in silica microspheres without CuS/Cu$_2$O/CuO-GO nanocomposites and the Raman spectrum appeared with lower underlying continuum than in MB system. However, Raman spectra of silica microspheres with nanocomposites reveal the presence of small multiple Raman peaks from Si(OC$_2$H$_5$)$_4$ and D and G bands from GO, indicating that CuS/Cu$_2$O/CuO-GO nanocomposites are inside the silica network at the close contact with the oil phase. In these spectra no peaks from MG were observed. We assume that the charge transfer process between MG and CuS/Cu$_2$O/CuO-GO can be prevented by the oil phase. We believe that success of the ultrasonic encapsulation of MG into the oil phase can be of interest in drug delivery applications, in which organic drug molecules are encapsulated into the oil-core surrounded by the protective silica@CuS/Cu$_2$O/CuO-GO shell enabling controlled release properties at the nanoscale.

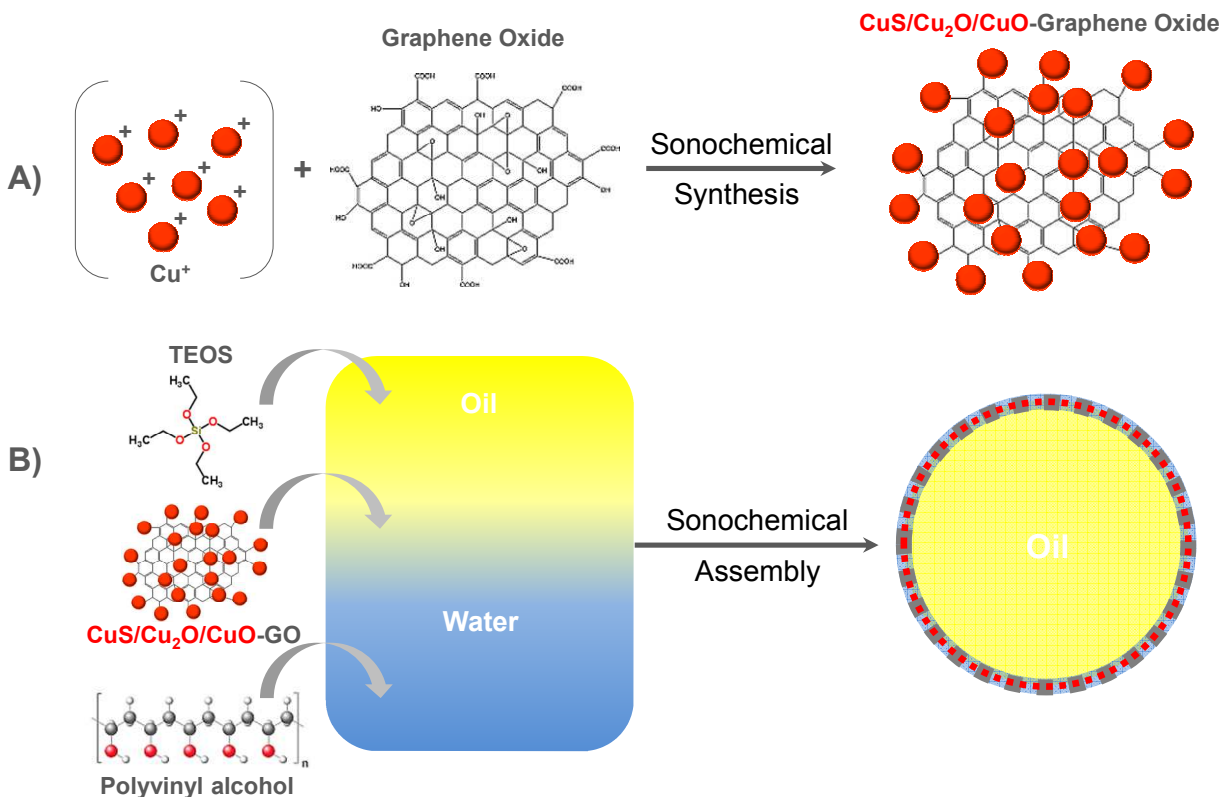### 4. Conclusions

We successfully developed a new sonochemical method for the synthesis of novel CuS/Cu$_2$O/CuO-GO nanocomposites with advanced charge carrier properties due to the presence of three copper phases such as CuS/Cu$_2$O/CuO in individual graphene oxide. DLS showed the monomodal homogeneous distribution of these nanocomposites with submicron size if the concentration of copper is increased by five times. The presence of p-type semiconductor covellite CuS, a Bloch p-type semiconductor cuprite Cu$_2$O and Cu bis-μ-oxo dimer in individual nanocomposites was revealed by Raman microscopy and X-Ray powder diffraction analysis and also confirmed by the UV-Vis absorption and FT-IR spectroscopy. We demonstrated that these

CuS/Cu$_2$O/CuO-GO nanocomposites could be used for the sonochemical assembly of stable oil-filled microspheres in the presence of polyvinyl alcohol (PVA) and tetraethyl orthosilicate (TEOS). We found out that such microspheres emitted visible light of different colors: green, yellow and red when dispersed in water. This photoluminescence property of microspheres appeared as a result of H-bridging between PVA and CuS/Cu$_2$O/CuO-GO nanostructure as well as light absorption ability of Cu$_2$O and charge transfer insulator CuO. Substitution of PVA by organic dye (methylene blue, MB, or malachite green, MG) led to strong fluorescence quenching of MB adsorbed on CuS/Cu$_2$O/CuO-GO nanocomposite within the silica network, as a result of induced charge transfer. In contrast, MG was encapsulated rather in the oil phase than in the silica@CuS/Cu$_2$O/CuO-GO nanocomposite and charge transfer was not induced. This effect of charge transfer inhibition resulted from poor interaction between MG and CuS/Cu$_2$O/CuO-GO nanostructure because MG adapted a non-ionized form in a basic medium, which favors interaction with the oil phase.

Scheme 1. 1) Schematic illustration of sonochemical synthesis of CuS/Cu$_2$O/CuO-GO nanocomposites from graphene oxide (GO), CuCl$_2$ (at 25×10^{-3} mol·L^{-1}) and Na$_2$S (at 1 mol·L^{-1}) by using ultrasonic horn type dispergator (20 kHz) in sequential sonication at 8 W/cm^2 as the first step and 18 W/cm^2 as the second step. 2) Scheme of the proposed sonochemical assembly method for the preparation of oil-filled silica@CuS/Cu$_2$O/CuO-GO microspheres via 3 min of ultrasonic emulsification (20 kHz, 27 W/cm^2) of a biphasic mixture consisting of organic phase (sunflower oil and tetraethyl orthosilicate) and aqueous phase (CuS/Cu$_2$O/CuO-GO nanocomposites and 5 wt.% polyvinyl alcohol).
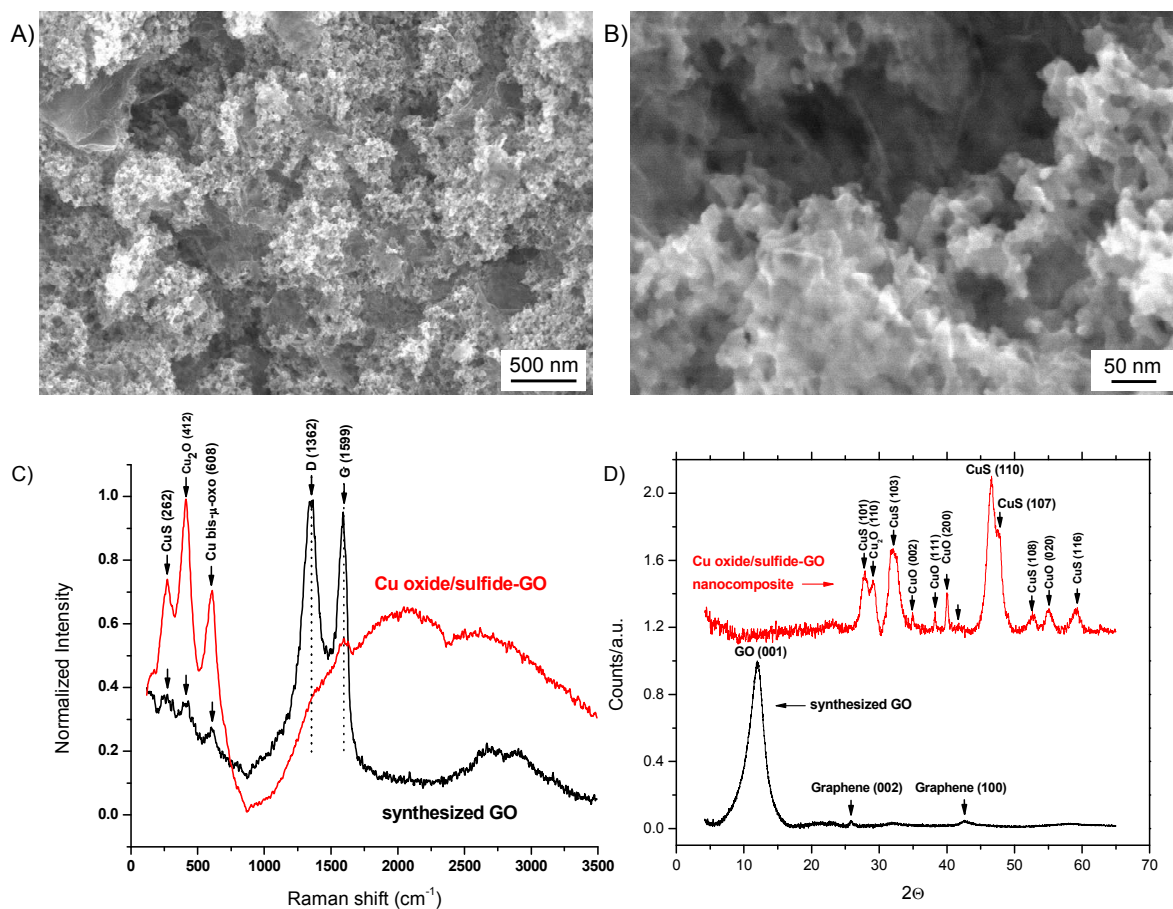
Figure 1. A) Representative SEM image of CuS/Cu$_2$O/CuO-GO nanocomposites, which were sonochemically prepared from graphene oxide (GO) nanosheets (synthesized by Hummers method), 25x10^{-3} mol·L^{-1} CuCl$_2$ and 1 mol·L^{-1} Na$_2$S by using ultrasound (20 kHz, at 8 W/cm^2 intensity as the first step and 18 W/cm^2 intensity as the second step) (scale bar is 500 nm). B) Enlarged SEM image of these nanocomposites (scale bar 50 nm). C) Raman spectra of sonochemically prepared CuS/Cu$_2$O/CuO-GO nanocomposites at 2x10^{-3} W (red line) and 6x10^{-3} W (black line) laser power and 633 nm excitation wavelength. At least five spectra were collected with 10 s of integration time for an individual spectrum acquisition. D) X-Ray powder diffraction patterns of synthesized GO (in black) and CuS/Cu$_2$O/CuO-GO nanocomposites (in red).
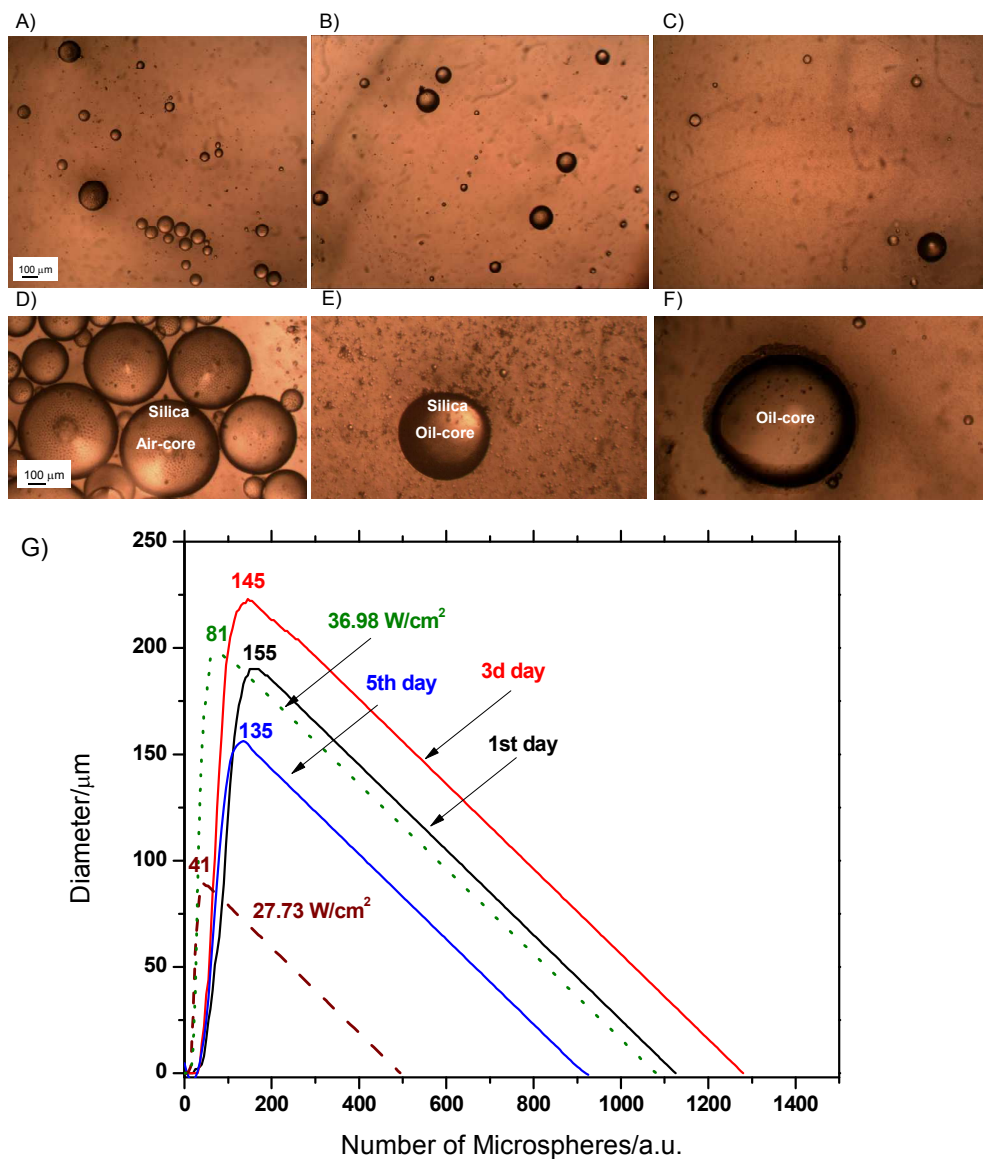
Figure 2. Representative optical phase contrast microscope images of sonochemically prepared CuS/Cu$_2$O/CuO-GO microspheres by using A) tetraethyl orthosilicate (TEOS) as silica precursor; B) the mixture of TEOS and sunflower oil at a volume ratio 1:1; C) sunflower oil as a single organic phase. CuS/Cu$_2$O/CuO-GO microspheres in B) and C) were prepared with 5 wt.% polyvinyl alcohol as the aqueous phase. Ultrasonic horn type dispergator, operating at 20 kHz

frequency and 27 W/cm^2 intensity, was employed for 3 min of sonochemical assembly of three types of microspheres containing D) silica and air-core, E) silica and oil-core and F) oil-core. F) Diagram of diameter distribution (μm scale, ± 5 nm) of sonochemically prepared silica@CuS/Cu$_2$O/CuO-GO microspheres obtained from the optical microscope images as average of five experiments being carried out on the first day (solid black line) of synthesis and after aging in mother-liquor solution for two (solid red line) and five (solid blue line) days as indicated by arrows. Two other diagrams of average diameter distribution indicate silica@CuS/Cu$_2$O/CuO-GO microspheres, which were sonochemically formed at 27.73 W/cm^2 (brown dashed line) and 36.98 W/cm^2 (green dotted line indicated by arrow).
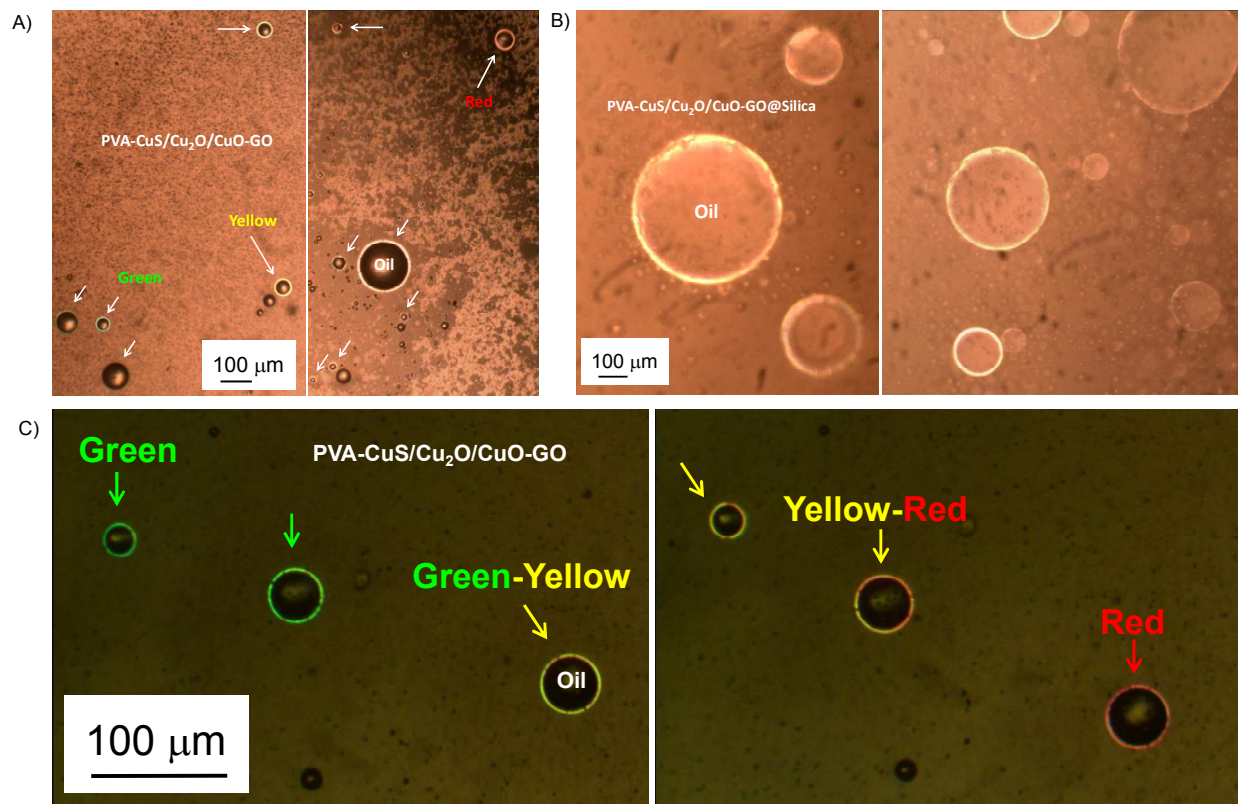
Figure 3. Representative optical phase contrast images of sonochemically prepared oil-filled CuS/Cu₂O/CuO-GO microspheres with polyvinyl alcohol (PVA-CuS/Cu$_2$O/CuO-GO): A) and C) these microspheres without TEOS and B) with TEOS. PVA-CuS/Cu$_2$O/CuO-GO microspheres in A) and C) were stored at room temperature and emit intense green, yellow and red light. PVA-silica@CuS/Cu$_2$O/CuO-GO microspheres in B) were obtained after 2 h heat treatment at 100°C and emit bright yellow color.
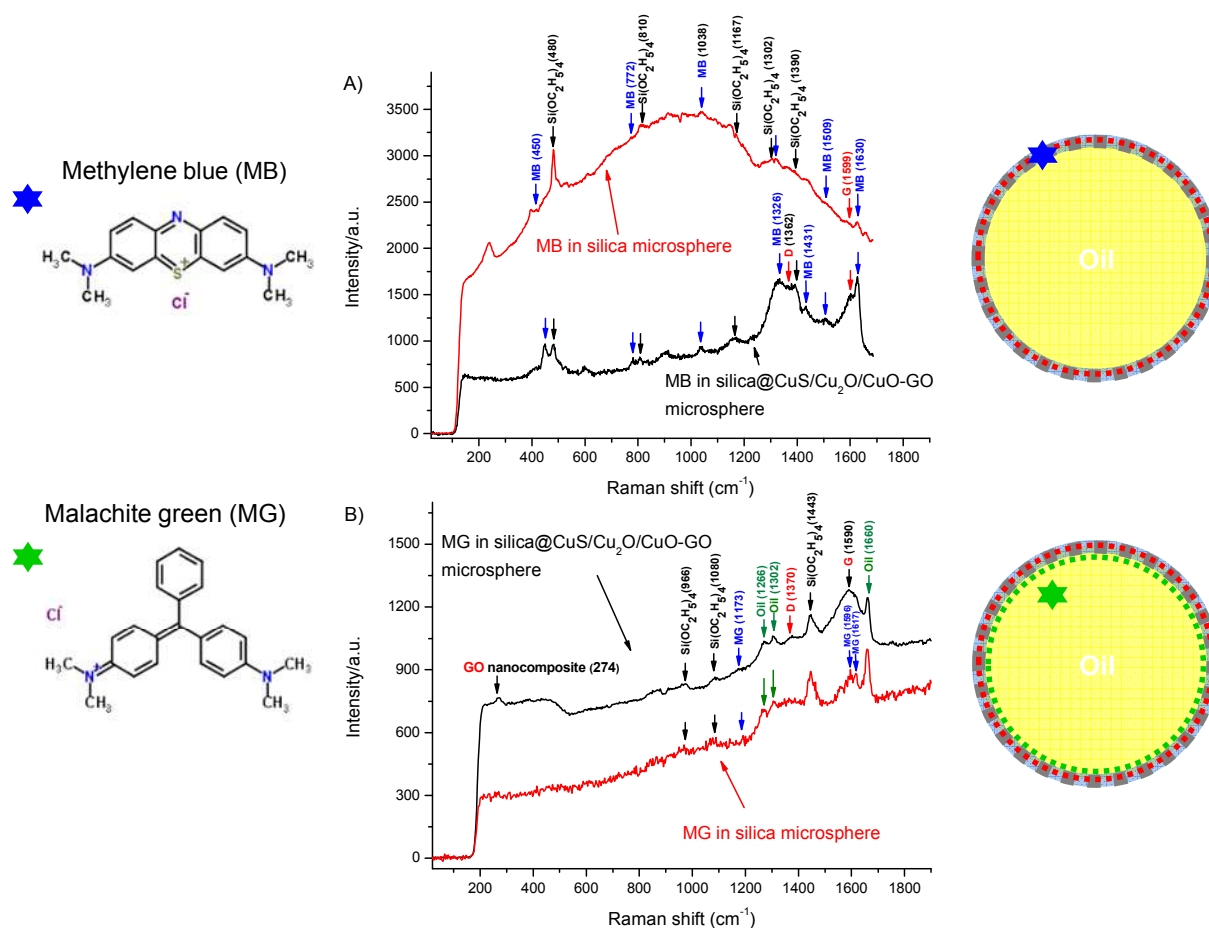
Figure 4. Raman spectra of oil-filled silica microspheres (red line) and silica@CuS/Cu₂O/CuO-GO microspheres (black line) with encapsulated organic dye molecules: A) methylene blue (MB) and B) malachite green (MG). Raman spectra were collected at $2x10^{-3}$ W of laser power and 633 nm excitation wavelength and 10 s of integration time by using inverted confocal Raman microscope Confotec NR500. At least five spectra were collected with 10 s of integration time for an individual spectrum acquisition.

Supporting Information. Detailed experimental procedures, more EDX spectra and tables with elemental composition, SEM images; UV-Vis absorption, FT-IR and Raman spectra; Zeta potential and DLS diagrams; optical phase contrast images. This material is available free of charge via the Internet at http://pubs.acs.org.

Funding Sources

REFERENCES

1   Pelaz, B.; Alexiou, C.; Alvarez-Puebla, R. A.; Alves, F.; Andrews, A.M.; et. al. Diverse Applications of Nanomedicine. *ACS Nano* **2017**, *11*, 2313–2381.

2   Sanchez-Iglesias, A.; Claes, N.; Soles, D. M.; Taboada, J. M.; Bals, S.; Liz-Marzan, L. M.; Grzelczak, M. Reversible Clustering of Gold Nanoparticles under Confinement. *Angew. Chem. Int. Ed.* **2018**, *57*, 3183–3186.

3   Sreejith, S.; Ma, X., Zhao, Y., Graphene Oxide Wrapping on Squaraine-Loaded Mesoporous Silica Nanoparticles for Bioimaging. *J. Am. Chem. Soc.* **2012**, *134*, 17346–17349.

4   Torres, T. Graphene Chemistry. *Chem. Soc. Rev.* **2017**, *46*, 4385–4386.

5   Eda, G.; Lin, Y. Y.; Mattevi, C.; Yamaguchi, H.; Chen, H. A.; Chen, I. S.; Chen, C. W.; Chhowalla, M. Blue Photoluminescence from Chemically Derived Graphene Oxide. *Adv. Mater.* **2010**, *22*, 505−550.

6   Zheng, P.; Wu, N. Fluorescence and Sensing Applications of Graphene Oxide and Graphene Quantum Dots: A Review. *Chem. Asian J.* **2017**, *12*, 2343–2353.

7   Galande, C.; Mohite, A. D.; Naumov, A. V.; Gao, W.; Ci, L.; Ajayan, A.; Gao, H.; Srivastava, A.; Weisman, R. B.; Ajayan, P. M. Quasi-Molecular Fluorescence from Graphene Oxide. *Sci. Rep.* **2011**, *1*, 85, 1−5.

8   Kochmann, S.; Hirsch, T.; Wolfbeis, O. S. The pH Dependence of the Total Fluorescence of Graphite Oxide. *J. Fluoresc*. **2012**, *22*, 849−855.

9   Lim, Y. F., Chua, C. S., Lee, C. J.; Chi, D. Sol-Gel Deposited Cu_2O and CuO Thin Films for Photocatalytic Water Splitting. *Phys. Chem. Chem. Phys*. **2014**, *16*, 25928–25934.

10 Dubale, A. A.; Tamirat, A. G.; Chen, H.-M.; Berhe, A. T.; Su, W.-N.; Hwang, B.-J. A Highly Stable CuS and CuS–Pt Modified Cu_2O/CuO Heterostructure as an Efficient Photocathode for the Hydrogen Evolution Reaction. *J. Mater. Chem. A* **2016**, *4*, 2205–2216.

11 Liu, Z.; Bai, H.; Xu, S.; Sun, D. D. Hierarchical CuO/ZnO "Corn-Like" Architecture for Photocatalytic Hydrogen Generation. *Int. J. Hydrogen Energy* **2011**, *36*, 13473–13480.

12 Wang, P.; Wen, X.; Amal, R.; Ng, Y. H. Introducing a Protective Interlayer of TiO_2 in Cu_2O–CuO Heterojunction Thin Film as a Highly Stable Visible Light Photocathode. *RSC Adv.* **2015**, *5*, 5231–5236.

13 Huang, Q., Kang, F., Liu, H., Li, Q.; Xiao, X. Highly Aligned Cu_2O/CuO/TiO_2 Core/Shell Nanowire Arrays as Photocathodes for Water Photoelectrolysis. *J. Mater. Chem. A* **2013**, *1*, 2418–2425.

14 Grinberg, O.; Shimanovich, U.; Gedanken, A. Encapsulating Bioactive Materials in Sonochemically Produced Micro- and Nano-Spheres. *J Mater. Chem. B* **2013**, *1*, 595–605.

15 Shi, J.; Zhou, X.; Liu, Y.; Su, Q.; Zhang, J.; Du, G. Sonochemical Synthesis of CuS/reduced Graphene Oxide Nanocomposites with Enhanced   Absorption and Photocatalytic Performance. *J. Mater. Res.* **2014**, *126*, 220–223.

16 Deng, Y.; Handoko, A. D.; Du, Y.; Xi, S.; Yeo, B. S. In Situ Raman Spectroscopy of Copper and Copper Oxide Surfaces during Electrochemical Oxygen Evolution Reaction: Identification of CuIII Oxides as Catalytically Active Species. *ACS Catalysis* **2016**, *6*, 2473–2481.

17 Karikalan, N.; Karthik, R.; Chen, S.-M.; Karuppiah, C.; Elangovan, A. Sonochemical Synthesis of Sulfur Doped Reduced Graphene Oxide Supported CuS Nanoparticles for the Non-Enzymatic Glucose Sensor Applications. *Sci. Rep.* **2017**, *7*, 1–10.

18 Sardari, B.; Özcan, M. Real-Time and Tunable Substrate for Surface Enhanced Raman Spectroscopy by Synthesis of Copper Oxide Nanoparticles via Electrolysis. *Sci. Rep.* **2017**, *7*, 1–11.

19 Reina, G.; Gonzalez-Domınguez, J. M.; Criado, A.; Vazquez, E.; Bianco, A.; Prato, M. Promises, Facts and Challenges for Graphene in Biomedical Applications. *Chem. Soc. Rev.* **2017**, *46*, 4400–4416.

20 Shimanovich, U.; Eliaz, D.; Aizer, A.; Vayman, I.; Micheli, S.; Shav-Tal, Y.; Gedanken, A. Sonochemical Synthesis of DNA Nanospheres. *ChemBioChem* **2011**, *12*, 1678–1681.

21 Shimanovich, U.; Volkov, V.; Eliaz, D.; Aizer, A.; Michaeli, S.; Gedanken, A. Stabilizing RNA by the Sonochemical Formation of RNA Nanospheres. *Small* **2011**, *7*, 1068–1074.

22 Suslick, K. S.; Grinstaff, M. W. Protein Microencapsulation of Nonaqueous Liquids. *J. Am. Chem. Soc.* **1990**, *112*, 7809–7811.

23 Sametband, M.; Shimanovich, U.; Gedanken, A. Graphene Oxide Microspheres Prepared by a Simple, One-Step Ultrasonication Method. *New J. Chem.* **2012**, *36*, 36–39.

24 Grigoriev, D.; Miller, R.; Shchukin. D.; Möhwald, H. Interfacial Assembly of Partially Hydrophobic Silica Nanoparticles Induced by Ultrasonic Treatment. *Small* **2007**, *3*, 665–671.

25 Blanco, E.; Esquivias, L.; Litran, R.; Pinaro, M.; Ramirez-del-Solar, M.; de la Rosa-Fox, N. Sonogels and Derived Materials. *Appl. Organomet. Chem.* **1999**, *13*, 399–418.

26 Qian, X.; Emory, S. R.; Nie, S. Anchoring Molecular Chromophores to Colloidal Gold Nanocrystals: Surface-Enhanced Raman Evidence for Strong Electronic Coupling and Irreversible Structural Locking. *J. Am. Chem. Soc*. **2012**, *134*, 2000–2003.

27 Haubner, K.; Murawski, J.; Olk, P.; Eng, L. M.; Ziegler, C.; Adolphi, B.; Jaehne, E. The Route to Functional Graphene Oxide. *ChemPhysChem* **2010**, *11*, 2131–2139.

28 Hummers, Jr. W. S.; Offeman, R. Preparation of Graphitic Oxide. *J. Am. Chem. Soc*. **1958**, *80*, 1339–1339.

29 Margulis, M. A.; Margulis, I. M. Calorimetric Method for Measurement of Acoustic Power Absorbed in a Volume of a Liquid. *Ultrason. Sonochem.* **2003**, *10*, 343–345.

30 Radziuk, D.; Shchukin, D. G.; Skirtach, A.; Möhwald, H.; Sukhorukov, G. Synthesis of Silver Nanoparticles for Remote Opening of Polyelectrolyte Microcapsules. *Langmuir*, **2007**, *23*, 4612–4617.

31 Tucureanu, V.; Matei, A.; Avram, A. M. FTIR Spectroscopy for Carbon Family Study. *Crit. Rev. Anal. Chem*. **2016**, *46*, 502–520.

32 Henson, M. J.; Mukherjee, P.; Root, D. E.; Stack, T. D. P.; Solomon, E. I. Spectroscopic and Electronic Structural Studies of the Cu(III)2 Bis-í-oxo Core and Its Relation to the Side-On Peroxo-Bridged Dimer. *J. Am. Chem. Soc.* **1999**, *121*, 10332–10345.

33 Hagemann, H.; Bill, H.; Sadowski, W.; Walker, E.; Francois, M. Raman Spectra of Single Crystal CuO. *Solid State Commun*. **1990**, *73*, 447–451.

34 Sumit Saxena, T. A. T.; Shukla S.; Negusse, E.; Chen, H.; Bai, J. Investigation of Structural and Electronic Properties of Graphene Oxide. *Appl. Phys. Lett*. **2011**, *99*, 013104-1-2.

35 Hsu, S.-W.; Bryks, W.; Tao, A. R. Effects of Carrier Density and Shape on the Localized Surface Plasmon Resonances of $Cu_{2-x}S$ Nanodisks. *Chem. Mater*. **2012**, *24*, 3765–3771.

36 Yang, Y.; Xu, D.; Wu, Q.; Diao, P. Cu_2O/CuO Bilayered Composite as a High-Efficiency Photocathode for Photoelectrochemical Hydrogen Evolution Reaction. *Sci. Rep*. **2016**, *6*, 1–13.

37 Ross, P. K.; Solomon, E. I. An Electronic Structural Comparison of Copper-Peroxide Complexes of Relevance to Hemocyanin and Tyrosinase Active Sites. *J. Am. Chem. Soc*. **1991**, 113, 3246–3259.

38 Bertoluzza, A.; Fagnano, C.; Morelli, M. A.; Gottardi, V.; Guglielmi, M. Raman and Infrared Spectra on Silica Gel Evolving toward Glass. *J. Non-Cryst. Solids* **1982**, *48*, 117–128.

39 Muika, B.; Lendl, B.; Molina-Dıaz, A.; Ayora-Canada, M. J. Direct Monitoring of Lipid Oxidation in Edible Oils by Fourier Transform Raman Spectroscopy. *Chem. Phys. Lipids* **2005**, *134*, 173–182.

40 Kim, J.; Cote, L. J.; Kim, F.; Yuan, W.; Shull, K. R.; Huang, J. Graphene Oxide Sheets at Interfaces. *J. Am. Chem. Soc.* **2010**, *132*, 8180–8186.

41 Radziuk, D.; Möhwald, H. Ultrasonically Treated Liquid Interfaces for Progress in Cleaning and Separation Processes. *Phys.Chem.Chem.Phys*. **2016**, *18*, 21–46.

42 Kundu, A.; Layek, R. K.; Kuila, A.; Nandi, A. K. Highly Fluorescent Graphene Oxide-Poly(vinyl alcohol) Hybrid: An Effective Material for Specific Au^{3+} Ion Sensors. *ACS Appl. Mater. Interfaces* **2012**, *4*, 5576–5582.

43 Galande, C.; Mohite, A. D.; Naumov, A. V.; Gao, W.; Ci, L.; Ajayan, A.; Gao, H.; Srivastava, A.; Weisman, R. B.; Ajayan, P. M. Quasi-Molecular Fluorescence from Graphene Oxide. *Sci. Rep.* **2011**, *1*, 1–5.

44 Tardivo, J. P.; Del Giglio. A.; de Oliveira, C. S.; Gabrielli, D. S.; Junqueira, H. C.; Tada, D. B.; et. al. Methylene Blue in Photodynamic Therapy: From Basic Mechanisms to Clinical Applications. *Photodiagn Photodyn Ther*. **2005**, *2*, 175–191.

45 Alderman, D. J. Malachite Green: a Review. *J. Fish Diseases* **1985**, *8*, 289–298.

Table of Contents Graphic (TOC)
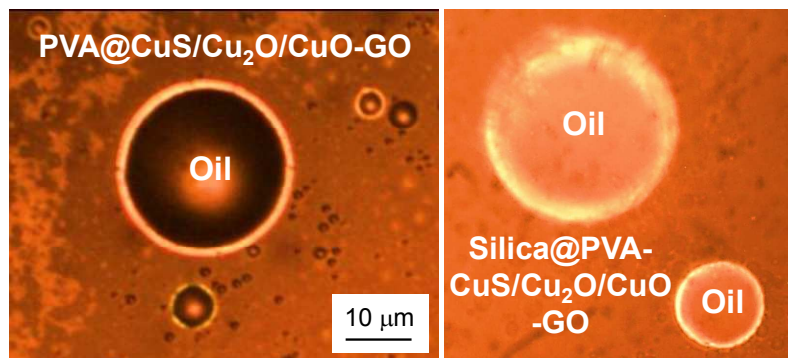
Photoluminescent oil-filled microspheres can be prepared through sonochemical assembly of a biphasic oil : water mixture containing amphiphilic $CuS/Cu_2O/CuO$-GO nanocomposites, tetraethyl orthosilicate or polyvinyl alcohol.